

TI DISTRIBUTION IN GRAIN-SIZE FRACTIONS OF APOLLO SOILS 10084 AND 71501.

W. G. Kong^{1,2}, B. L. Jolliff², and Alian Wang² ¹School of Physics, Shandong University, Jinan, China gavink@levee.wustl.edu ²Department of Earth and Planetary Sciences and the McDonnell Center for the Space Sciences, Washington University, St. Louis, MO 63130 USA

Introduction: The ultraviolet-visible (UV-Vis) ratio is a widely used parameter to estimate the Ti distribution on the lunar surface, and new observations with the LRO wide-angle camera (WAC) are contributing to this effort with global measurements including bands at 321 and 360 nm [1]. To better understand the correlation between UV-Vis ratio and Ti content, we have been doing laboratory analyses of lunar soil samples using a combined digital imaging (backscattered electron image and X-ray maps) method to get quantitative results on abundances. In this study, we report on the Ti distribution in two Ti-rich soils, 10084 from Apollo 11 and 71501 from Apollo 17. The TiO₂ concentration of bulk soil 10084 ($I_s/FeO = 78$) is 7.3 wt% [3,4,5], and that of bulk soil 71501 ($I_s/FeO = 35$) is 9.5 wt% [3,4,6]. This work is a continuation of previous work reported by Johnson et al. [2]. The questions we are addressing include:

- (1) How is Ti distributed quantitatively among its mineral and lithologic hosts, including volcanic and impact glasses and agglutinates?
- (2) How does the Ti distribution vary among grain size fractions?
- (3) How does the Ti distribution vary with maturity?

Experiment and methods: Samples of 10084 and 71501 were each sieved into five different size fractions: >210 μm , 100-210 μm , 48-100 μm , 20-48 μm , and <20 μm . The analyses for 100-210 μm size fractions of 10084 and 71501 were reported in [2]. We include the analyses of 48-100 μm and 20-48 μm size fractions of both samples, and compare them with 100-210 μm size fraction.

Samples were mounted in epoxy grain mounts, polished, and analyzed using a JEOL 8200 electron microprobe. Two back-scattered electron (BSE) maps and 10 major-element X-ray maps were acquired on all six samples. Figure 1 shows the BSE map and related Ti X-ray map of three grain-size fractions from 71501.

Grains in the BSE and element X-ray maps were classified into eight classes, i.e., basalt, breccia, agglutinates, plagioclase, ilmenite, pyroxene, olivine, and glass. By this classification, we track lithic components such as basalt and breccia as well as crystalline mineral and glass components because we are interested in how these particles break down. Each grain was individually examined and classified. The area and shape of each grain were analyzed using ImageJ software. The shape of these grains is defined by the aspect ratio (AR, major axis/minor axis) as follows: AR

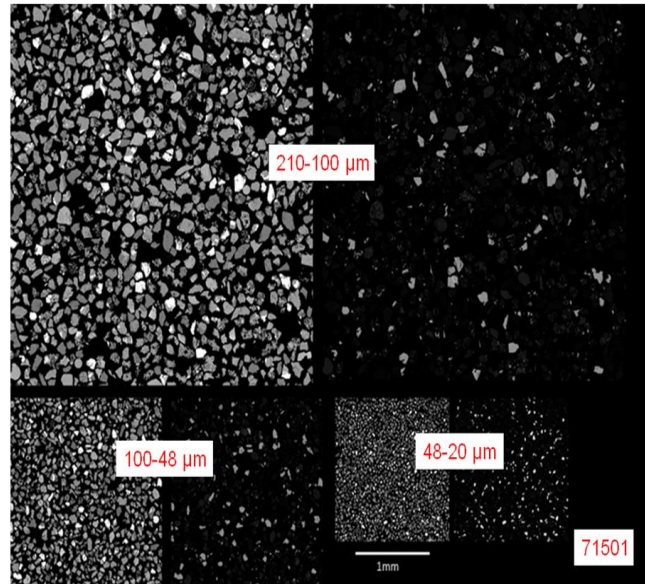


Figure 1. BSE images (left) and Ti X-ray images (right) of the three grain size fractions of sample 71501. In X-ray image, brightness reflects the Ti concentration. The bright grains are mostly ilmenite and grey grains are mostly Ti-bearing glasses.

of 1:1, equant; AR of 2:1 to 1:1, blocky; 5:1 to 2:1, tabular; and > 5:1, acicular. About one thousand grains of each grain size fraction of each soil sample were studied.

Results and discussion: The results of mineral and lithologic modal analysis of samples are shown in figure 2. The most abundant components in both soils are

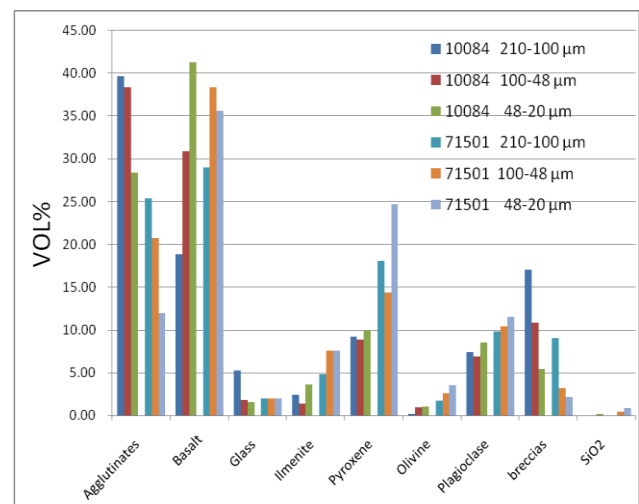


Figure 2. Bar presentation of mineral and lithologic modal analysis of three grain-size fractions of lunar soils 10084 and 71501.

agglutinates and basalt fragments, which together account for 60-70 Vol. %. These values compare well with results of previous studies [7-9]. We find the volume % of agglutinates to decrease with decreasing grain size through these size fractions. However, in the finer fractions (45-20 μm fraction?), Taylor et al. [10] find this trend reverses.

Mass-balance calculation. Although it might seem intuitive to equate the Ti content of lunar soils with ilmenite abundance, this is not strictly the case. We use a mass-balance calculation coupled with results of our modal analysis to investigate the Ti distribution among mineral and lithic components. Results (Fig. 3) show that most of the Ti in 10084 and 71501 is hosted in free ilmenite or basalt grains (in basalt grains, most but not all of the Ti is also in ilmenite). In 71501, about 80-90 wt% of the Ti is in free ilmenite and basalt grains, with more Ti in ilmenite. In 10084, basalt and ilmenite host about 65-85 wt% of the Ti, with basalt grains hosting more Ti than free ilmenite grains. In 10084, 10-20% occurs in agglutinates, and in 71501, a less mature soil, ~4-10%. Ti in glasses, breccias, and pyroxene sum to ~10% or less in both soils.

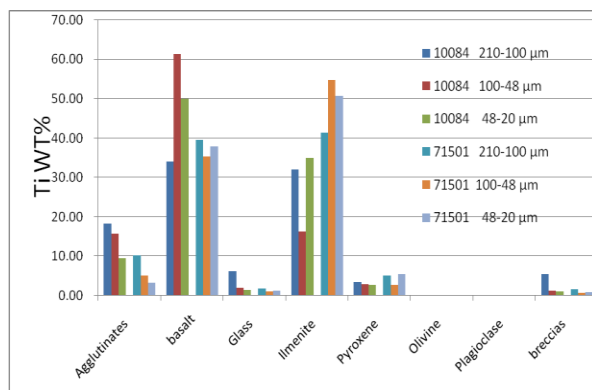


Figure 3. Bar presentation of Ti distributions among its mineral and lithologic hosts for three grain-size fractions of lunar soils 10084 and 71501.

Grain Shape Analysis. The results of grain shape analysis are listed in Table 1 for 10084 and Table 2 for 71501. In both soils the shape (by volume) of ilmenite grain is dominated by equant and blocky forms. In the mature lunar soil 10084, the shape of ilmenite grains shows a subtle trend to increased AR values (decrease of equant shape with increase of blocky & tabular

Table 1. Ilmenite grain shape analysis of 10084.

Shape	Grain size 210-100 μm	Grain size 100-48 μm	Grain size 48-20 μm
equant	45.90	39.20	35.01
blocky	35.60	38.47	44.24
tabular	17.40	19.48	19.66
acicular	1.08	2.85	1.09

Table 2. Ilmenite grain shape analysis of 71501.

Shape	Grain size 210-100 μm	Grain size 100-48 μm	Grain size 48-20 μm
equant	38.00	44.82	34.67
blocky	25.40	20.81	29.43
tabular	33.90	32.95	34.50
acicular	2.64	1.42	1.40

shapes) as grain size decreases. However, in the submature 71501, no clear trend was found.

Conclusions: The dominant Fe-Ti oxide mineral in 10084 and 71501 is ilmenite; other Ti-rich oxides (armalcolite, ulvöspinel, rutile) are very scarce. In both soils, the volume percent of agglutinates and breccias decreases as grain-size fractions decrease, and the volume percentages of single mineral grains have a consistent trend to increase as grain-size fractions decrease. This trend results from breakdown of breccias and basalt lithic fragments into finer, single mineral grains.

In mature soil 10084, more Ti is hosted in basalt as fine-grained ilmenite compared to the coarse, free ilmenite grains. In submature soil 71501, Ti is hosted mostly by coarse-grained ilmenite. This difference likely reflects initial basalt (ilmenite) characteristics.

No unique trend was found on the Ti content distribution variation among these grain-size fractions, whereas the ilmenite shape in mature soil 10084 shows a subtle trend.

Future work will include the analysis of <20 μm grain fraction to compare with these results and that of [10]. We will analyze additional lunar soils that cover a range of Ti concentrations (Apollo 12, Apollo 15) and levels of maturity. Subsequently, coupling our results and those of [10], we will compare results from the quantitative sample petrography to the UV-Vis spectra of the grain-size fractions to determine correlations between the Ti distribution and the UV-Vis ratio.

Acknowledgements: We thank Randy Korotev and Ryan A. Zeigler for providing their expertise and instructions to Weigang Kong. We also thank the Chinese Educational council for the scholarship to support the study of Weigang Kong at Washington University in St. Louis.

References: [1] Robinson, M. et al. (2011) this Conf.; [2] Johnson et al. (2008) LPS XXXX Abstr. # 2346 [3] Morris, R. V. (1978) *Proc. Lunar Planet Sci. Conf. 9th*, 2287- 2297. [4] Morris, R. V., et al. (1983) *Handbook of Lunar Soils*, NASA JSC, Houston. [5] Laul, J. C. and Papike, J. J. (1980) *Proc. Lunar Planet. Sci. Conf. 11th*, 2, 1307-1340. [6] Apollo 17 P.E.T (1973) *Science*, 182, 659-672. [7] Heiken, G. H., and D. S. McKay (1974) *Proc. Lunar Sci. Conf. 5th*, 843-860. [8] Simon, S. B., et al. (1981) *Proc. Lunar Planet. Sci. 12B.*, 371-388. [9] Taylor, L. A. et al. (1996) *Icarus*, 124, 500-512. [10] Taylor, L. A. et al. (2001) *J. Geophys. Res.*, 106, 27,985-27,999.